Kinetic analysis of crystal violet adsorption on to bottom ash

Puthiya Veetil NIDHEESH, Rajan GANDHIMATHI[*],
Sreekrishnaperumal Thanga RAMESH, Tangappan Sarasvathy ANANTHA SINGH
Department of Civil Engineering, National Institute of Technology, Tiruchirappalli,
620 015, Tamilnadu-INDIA
e-mail: rgmathii@nitt.edu

Abstract

The adsorption behavior of crystal violet (CV) from aqueous solution onto bottom ash was investigated under various experimental conditions. The parameters studied included contact time, initial CV concentration, particle size, and ionic strength. The kinetic experimental data were analyzed by different models. The experimental adsorption data showed good correlation with the kinetic models and suggested a multimechanism sorption process. The adsorption mechanisms follow pseudo-second-order kinetics with a significant contribution of intraparticle diffusion and film diffusion. Pseudosecondorder kinetics follows the removal of CV by bottom ash for smaller particle size (<150 μm) but the kinetics follows first order in the case of bottom ash size >150 μm. The adsorption mechanism was further analyzed by Reichenberg's method. The adsorption capacity of bottom ash decreases with increases in CV concentration and increases with particle size. The effect of ionic strength was analyzed by adding NaCl and CaCl$_2$. The ionic strength variation study showed that CV removal increases with increases in NaCl and CaCl$_2$ concentration.

Key Words: Adsorption, crystal violet, bottom ash, kinetics, kinetic models

1. Introduction

Dye pollutants are a major source of environmental contamination and color is the first contaminant to be recognized in wastewater (Banat et al., 1996). Textile companies, dye manufacturing industries, paper and pulp mills, tanneries, electroplating factories, distilleries, food companies, and a host of other industries discharge colored wastewater (McKay et al., 1998). Over 100,000 dyes have been made and more than 7×10^5 t are produced annually (McMullan et al., 2001). More than 10,000 dyes are commercially available and 5%-10% of these are discharged into wastewaters by textile industries (Gong et al., 2005). The presence of very small amounts of dyes in water (less than 1 mg/L for some dyes) is highly visible and undesirable (Banat et al., 1996; Robinson et al., 2001). The dye containing colored wastewater damages the aesthetic nature of water and enhances the chances of toxic impact on the aquatic flora and fauna. These water-soluble dyes offer considerable resistance for their biodegradation due to their complex structures and high thermal and photostability. Hence,

[*]Corresponding author

removal of dyes from wastewaters using economical means has become a real challenge to global scientists (Gupta et al., 2009).

Amongst the numerous techniques of dye removal, adsorption is the procedure of choice and gives the best results as it can be used to remove different types of coloring materials (Derbyshire et al., 2001; Ho and McKay, 2003; Jain et al., 2003). The major advantages of an adsorption treatment for the control of water pollution are less investment in terms of initial development cost, simple design, easy operation, and no or less generation of toxic substances. If the adsorption system is designed correctly it will produce a high-quality treated effluent (Crini, 2006). Adsorption onto activated carbon has been found to be superior for wastewater treatment compared to other physical and chemical techniques, such as flocculation, coagulation, precipitation, and ozonation, as they possess inherent limitations, such as high cost, formation of hazardous by-products, and intensive energy requirements (Padmesh et al., 2006). In the adsorption techniques, commercial activated carbon is a preferred adsorbent for color removal, but its widespread use is restricted due to its high cost (Xing et al., 2010). As such, alternative nonconventional sorbents have been investigated. It is well known that natural materials, waste materials from industry and agriculture, and biosorbents can be obtained and employed as inexpensive sorbents (Crini, 2006). The use of unconventional adsorbent has the following features (Weng and Pan, 2007): (1) it can be obtained abundant locally and cheaply. Most of them are readily to be utilized; (2) regeneration of these low-cost substitutes is not necessary whereas regeneration of activated carbon is essential. Such regeneration may result in additional effluent and the adsorbent may suffer considerable loss; (3) less operation cost in terms of maintenance and supervision is required for the unconventional adsorption systems; (4) utilization of industrial solid waste for the treatment of industrial wastewater is helpful not only to the environment, but also to reduce the disposal cost. Bottom ash is one of such low cost adsorbents. It is a coarse, granular, incombustible by-product of power plants, obtained after combusting coke. It is an undesired collected material, whose disposal has always been a matter of concern to the station authorities, as the dumped ash makes the land infertile (Hecht and Duvall, 1975).

Based on the above viewpoints, bottom ash was investigated for its potential use as adsorbent for the removal of crystal violet (CV) from aqueous solution. CV, also known as Basic Violet 3, is a well-known cationic dye being used for various purposes: a biological stain, a dermatological agent, a veterinary medicine, an additive to poultry feed to inhibit propagation of mold, intestinal parasites, and fungus etc. It is also extensively used in textile dying and paper printing (Adak et al., 2005). Parameters affecting the adsorption process such as initial dye concentration, contact time, adsorbent size, and ionic strength were evaluated in this study. Kinetic models were used for evaluating the mechanism and behavior of CV adsorption onto bottom ash.

2. Materials and methods

2.1. Adsorbent and adsorbate

The thermal power plant waste material bottom ash was utilized as potential adsorbent in this study. The adsorbent was obtained from Neyveli Lignite Corporation Limited, Neyveli, Tamilnadu, India. CV (A.R. Grade, C.I. 42,555, λmax = 579 nm, molecular weight = 407.99 g/mol, molecular formula = $C_{25}H_{30}ClN_3$), from S.D. Fine Chem. Pvt Ltd. was the adsorbate used for this study. The chemical structure of CV is shown in Figure 1.
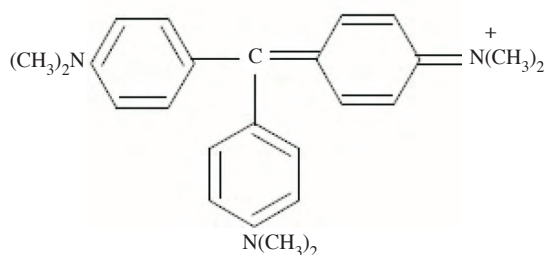
Figure 1. Chemical structure of CV (Mittal et al., 2010).

2.2. Characterization of adsorbent

Iodine number was determined according to the procedure given in the Process Design Manual for Carbon Adsorption, US Environmental Protection Agency. Iodine number measures the volume present in pores from 10-28 Å diameters (Benfield et al., 1982). Elemental analysis was determined by wet chemical method and measurement of elemental concentration was done by using an atomic absorption spectrophotometer (AAS) supplied by PerkinElmer, USA, Model AAnalyst 700. The loss on ignition (LOI) was determined by heating a pre-weighed dry sample (left at 105 °C in an oven and then cooled in desiccators) to 600 °C over 2 h (Bayat, 2002).

The point of zero charge (PZC) was determined using the solid addition method (Oladoja and Aliu, 2009) viz: into a series of 100 mL conical flasks 45 mL of 0.1 M KNO_3 solution was transferred. The pH values of the solution were roughly adjusted from 2 to 10 by adding either 0.1 N HNO_3 or NaOH. The total volume of the solution in each flask was made exactly 50 mL by adding the KNO_3 solution. The pH values of the solutions were then accurately noted. Bottom ash (1 g) was added to each flask which securely capped immediately. The suspension was then manually agitated. The pH values of the supernatant liquid were noted. The difference between the initial and final pH (pH_f) values ($\Delta pH = pH$ - pH_f) was plotted against the pH. The point of intersection of the resulting curve with pH gave the PZC.

Scanning electron microscopy (SEM) analysis was carried out for bottom ash to study its surface textures. The SEM analysis was done at $80\times$ magnification. In addition, the surface functional groups of bottom ash were detected by Fourier Transform Infrared (FTIR) Spectroscope (FTIR-2000, Perkin Elmer) using the KBr pellet method. The spectra were recorded from 4000 to 400 cm^{-1}.

2.3. Batch studies

Batch adsorption kinetic studies were performed in a set of Erlenmeyer flasks (250 mL) where solutions of dye (100 mL) with different initial concentrations (10-40 mg/L) were placed. Equal mass of bottom ash (50 mg of particle size 75-150 μm) was added to CV solutions and they were kept in an isothermal shaker (30 °C) at an agitation rate of 150 rpm. The initial pH of the sample was 8.07. Samples were withdrawn at regular interval (5, 10, 15, 20, 30, 40, 50, 60, 75, 90, 120, and 150 min) from the shaker and filtered using Whatman filter paper (No. 42). Then they were analyzed in UV-Visible spectrophotometer for finding the CV concentration. A similar procedure was followed to find the effect of particle size on CV removal using another set of Erlenmeyer flasks containing 100 mL of CV solution (10 mg/L) with the same dose of bottom ash (50 mg) with different size fraction. The effect of salt concentration (ionic strength) on the amount of CV adsorbed or removed by bottom ash was analyzed over the NaCl or $CaCl_2$ amount ranging from 0 to 250 mg.

3.   Results and discussion

3.1.   Characterization of bottom ash

The elemental composition of bottom ash is given in Table 1. It can be observed that the SiO_2 and Al_2O_3 contents make up about 89% of the bottom ash. Iodine number of bottom ash was 396.02 mg/g. The moisture content and LOI value of the bottom ash sample used were 16.65% and 48.36%, respectively. The high value of LOI indicates that bottom ash contains more organic matter (Nidheesh et al., 2011). The results of the zero point of charge of the bottom ash (pH $_{PZC}$ = 6.2) are presented in Figure 2.

It was observed that at pH less than 6.2 the surface of the bottom ash is predominated by positive charges, while at pH greater than 6.2 the surface is predominated by negative charges (Nidheesh et al., 2011). The SEM micrograph of bottom ash sample at $80\times$ magnification depicted in Figure 3 shows that the surface of bottom ash is porous. It is evident that the bottom ash particles are spherical. Fine fly ash particles can also be observed from Figure 3, which all indicate a favorable texture for dye adsorption on the bottom ash surface (Nidheesh et al., 2011).

Table 1. Composition of bottom ash (Nidheesh et al., 2011).

S. no	Element oxide	Weight (%)
1.	Calcium oxide (CaO)	2.11
2.	Alumina (Al_2O_3)	23.49
3.	Silica (SiO_2)	65.22
4.	Iron oxide (Fe_2O_3)	3.59
5.	Magnesia (MgO)	0.60
6.	Sodium oxide (Na_2O)	0.21
7.	Others	4.78
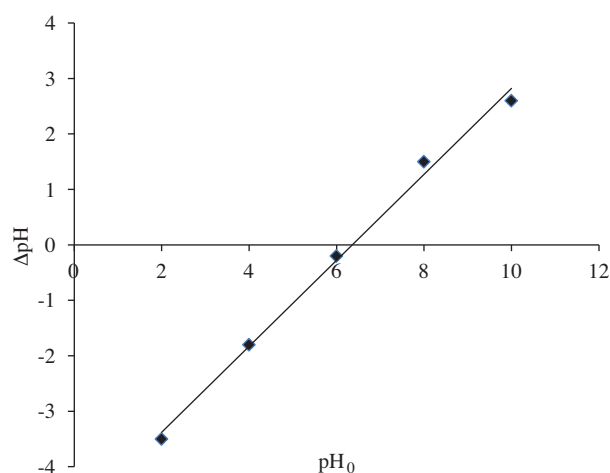
Figure 2. Point of zero charge for bottom ash (Nidheesh et al., 2011).

FTIR spectroscopy was carried out to identify the major functional groups presented in bottom ash and the results are shown in Figure 4. It was found that bottom ash has peaks at 953, 1098, 1638, 3451 cm^{-1} etc. The broad band around 3446 cm^{-1} was attributed to the surface hydroxyl groups, adsorbed water and amine groups. The O-H stretching vibrations occurred within a broad range of frequencies indicating the presence of

"free" hydroxyl groups and bonded O-H bands of carboxylic acids (Tan et al., 2008; Song et al., 2010). The band at 10001200 cm^{-1} reflects the siloxane (–Si–O–Si–) group, and the bands at 786 and 714 cm^{-1} represent SiO–H vibration (Lin et al., 2007).
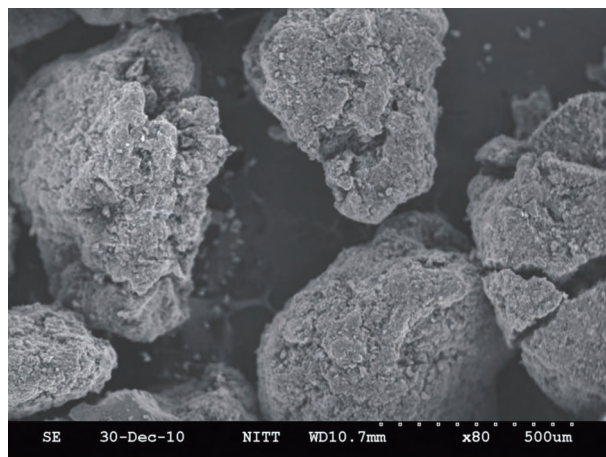

Figure 3. Micromorphology of bottom ash.

3.2. Effect of agitation time and initial concentration of dye on adsorption

A series of contact time experiments for the CV removal with bottom ash were carried out at different initial concentrations (10-40 mg/L) and at temperature of 30 °C, to find out the effect of initial dye concentration and contact time on the CV removal efficiency of bottom ash. This study was performed to determine the equilibrium time for maximum uptake at different CV concentrations. The results are shown in Figure 5.
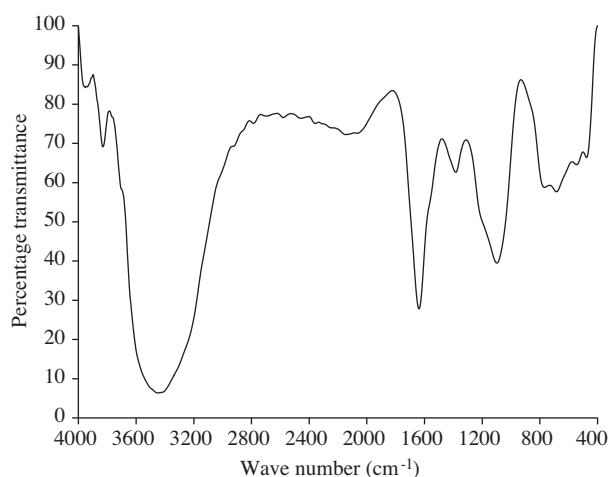

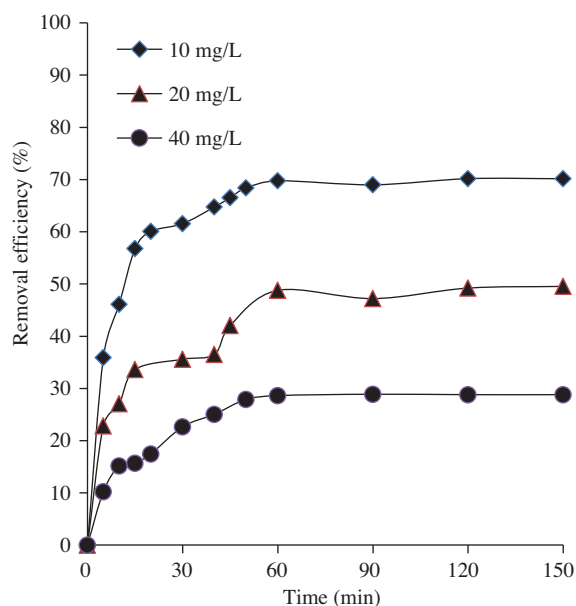**Figure 4.** FTIR spectrum of bottom ash (Nidheesh et al., 2011).

Figure 5. Effect of contact time and initial concentration on CV removal by bottom ash (size = 75-150 μm).

As can be seen from Figure 5, decolorization is extremely rapid in the first 15 min and the amount of CV adsorbed onto the bottom ash increases with time. At some point of time, it reaches a constant value beyond which no more is removed from solution. At this point, the amount of the dye desorbing from the adsorbent is in a state of dynamic equilibrium with the amount of the dye being adsorbed onto the bottom ash. The time required to attain this state of equilibrium is termed the equilibrium time, and the amount of dye adsorbed at the equilibrium time reflects the maximum adsorption capacity of the adsorbent under those operating conditions (Bello et al., 2010). This equilibrium was established at 60 min for all concentrations.

As can be seen in Figure 5, when the initial CV concentration was increased, the adsorption efficiency of bottom ash decreased, but the actual amount of CV adsorbed per unit mass of bottom ash increased with increase in CV concentration (Table 2). The adsorption efficiency of bottom ash decreased from 69.78% to 28.6% as the initial CV concentrations increased from 10 to 40 mg/L, but the adsorption capacity of bottom ash increased from 6.978 to 11.446 mg/g for the above condition. This is because at lower concentration the ratio of the initial number of dye molecules to the available surface area is low; subsequently, the fractional adsorption becomes independent of the initial concentration. However, at high concentration the available sites of adsorption become fewer, and hence the percentage removal of dye is dependent upon the initial concentration (Hema and Arivoli, 2007).

3.3. Kinetic studies

The kinetics of basic dyes sorption was investigated using different models, as given below:

Pseudo-first-order equation (Lagregren, 1898):

$$\log (q_e - q_t) = \log (q_e) - \frac{k_1}{2.303} t \tag{1}$$

Second-order Lagergren equation (Ho and McKay, 1999):

$$\left(\frac{t}{q_t} \right) = \frac{1}{k_2 q_e^2} + \frac{1}{q_e} (t) \tag{2}$$

Elovich equation (Chien and Clayton, 1980):

$$q_t = \frac{\ln (\beta \alpha)}{\beta} + \frac{\ln t}{\beta} \tag{3}$$

Natarajan and Khalaf (Kannan and Vanangamudi, 1991):

$$\log \left(\frac{C_0}{C_t} \right) = \frac{k}{2.303} t \tag{4}$$

Bhattacharya-Venkobachar (Bhattacharya and Venkobachar, 1984):

$$\log [1 - U (T)] = -\frac{k_B}{2.303} t \tag{5}$$

where

$$U (T) = \frac{C_0 - C_t}{C_0 - C_e} \tag{6}$$

Table 2. Adsorption kinetic model rate constants for CV removal.

Parameters	CV concentration (mg/L)			Particle size (μm)			
	10	20	40	<75	75-150	150-300	300-600
q_e exp (mg/g)	6.978	9.761	11.446	8.985	6.978	5.638	2.310
Removal efficiency (%)	69.78	48.8	28.6	89.85	69.78	56.38	23.1
Pseudo-first-order model							
q_e (cal) (mg/g)	4.869	6.826	10.278	7.495	4.869	5.232	2.679
k_1 (min^{-1})	0.065	0.033	0.048	0.085	0.065	0.064	0.053
R^2	0.945	0.848	0.976	0.986	0.945	0.984	0.922
Pseudo-second-order model							
q_e (cal) (mg/g)	7.273	10.616	12.658	8.984	7.331	6.253	2.828
k_2 (g/mg/min)	0.0304	9×10^{-3}	9×10^{-3}	0.062	0.028	0.018	0.016
R^2	0.999	0.994	0.995	0.998	0.999	0.995	0.969
Intraparticle diffusion model							
K_{id} (mg/g min$^{0.5}$)	0.321	1.228	1.559	0.661	0.321	0.357	0.330
C	4.494	0.085	0.208	4.52	4.494	2.929	-0.214
R^2	0.949	0.903	0.991	0.957	0.949	0.961	0.943
Elovich equation							
α (mg/g min)	4.537	6.044	1.98	8.65	4.537	5.506	0.208
β (mg/g min)	0.742	0.65	0.326	0.614	0.742	0.969	1.204
R^2	0.958	0.923	0.962	0.989	0.958	0.987	0.905
Natarajan and Khalaf equation							
k (min^{-1})	0.0122	6.4×10^{-3}	4.1×10^{-3}	0.031	0.0122	0.011	0.0017
Intercept	0.238	0.109	0.0482	0.341	0.238	0.123	0.004
R^2	0.868	0.926	0.961	0.941	0.868	0.822	0.941
Bhattacharya and Venkobachar equation							
k_B (min^{-1})	0.065	0.026	0.0419	0.087	0.065	0.071	0.057
Intercept	−0.156	−0.247	−0.0992	−0.138	−0.156	0.047	0.135
R^2	0.945	0.86	0.945	0.992	0.945	0.94	0.899
Fractional power model							
a	2.534	3.134	2.098	3.976	2.534	2.435	0.243
b	0.262	0.247	0.423	0.2133	0.262	0.205	0.55
R^2	0.93	0.932	0.978	0.982	0.93	0.982	0.92
Film diffusion mass transfer rate equation							
R^1 (min^{-1})	0.0651	0.0329	0.0485	0.0847	0.0651	0.0697	0.053
Intercept	−0.359	−0.358	−0.107	−0.181	−0.359	0.058	0.148
R^2	0.946	0.848	0.976	0.986	0.946	0.96	0.922

Power function kinetic equation (Dalal, 1974):

$$\log q_t = \log a + b \log t \tag{7}$$

Intraparticle diffusion model (Weber and Morris, 1963):

$$q_t = k_{id} t^{1/2} + C \tag{8}$$

Film diffusion mass transfer rate equation (Boyd et al., 1947):

$$ln\,(1 - F) = -R^1 t \tag{9}$$

where

$$F = \frac{q_t}{q_e} \tag{10}$$

where q_e and q_t are the adsorption capacity at equilibrium and at time t, respectively (mg/g), k_1 is the rate constant of pseudo-first-order adsorption (1/min), k_2 is the rate constant of pseudo-second-order adsorption (g/mg/min), α is the initial adsorption rate (mg/g min) and β is the desorption constant (mg/g min), C and C_t are the concentrations of dye solution (in mg/L) at time zero (initial concentration) and at time t, $C_e =$ equilibrium dye concentration (mg/L), C is the intercept and k_{id} is the intraparticle diffusion rate constant (mg/g min$^{0.5}$), and R^1 (min^{-1}) is liquid film diffusion constant.

The above experimental results were also applied to different kinetic models and are shown in Figures 6-13. Parameters of all the models are given in Table 2. It can be seen that the linear correlation coefficients for the first-order and second-order model are good and based on the comparison between experimental and theoretically calculated q_e values, it was found that the pseudo-second-order model fitted better than pseudo-first-order model for removal of CV by bottom ash. Table 2 also shows that the rate of adsorption decreases with increase in initial CV concentration. The intraparticle diffusion plot (Figure 8) shows multilinearity between $t^{0.5}$ and q_t for the removal of CV by bottom ash. These results imply that the adsorption processes involve more than one single kinetic stage or sorption rate (Vaghetti et al., 2009). The intraparticle diffusion plot shows that the adsorption occurs in 3 steps. The first linear portion is the fastest step and is attributed to the diffusion of CV towards adsorbent. The second linear portion is a delay process that corresponds to intraparticle diffusion, but the intraparticle diffusion rate increases with initial CV concentration. The third stage is the diffusion through small pores and is followed by the establishment of equilibrium (Vaghetti et al., 2009). However, the experimental data at various initial CV concentrations were applied to the intraparticle diffusion kinetic model and the results are illustrated in Table 2. It is observed that the straight line of the intraparticle region did not pass through the origin and this indicates that the intraparticle diffusion is not the only rate-limiting step (Mohan and Singh, 2002). The correlation coefficients for the Elovich kinetic model (Figure 9) obtained at all the concentrations were very high, which may indicate that the diffusional rate-limiting is more prominent in CV sorption by bottom ash. However, Natarajan and Khalaf (Figure 10), Bhattacharya and Venkobachar (Figure 11) and film diffusion mass transfer rate plots (Figure 13) do not go through the origin. This reveals that the adsorption of CV onto bottom ash is a multistep process.
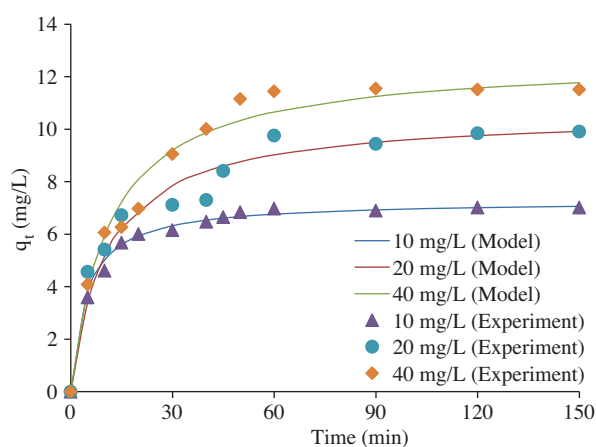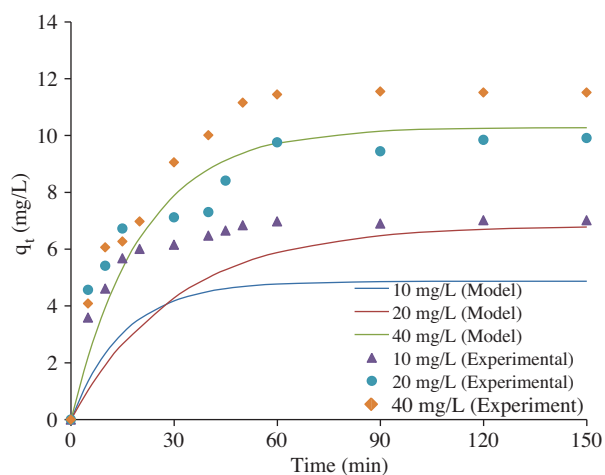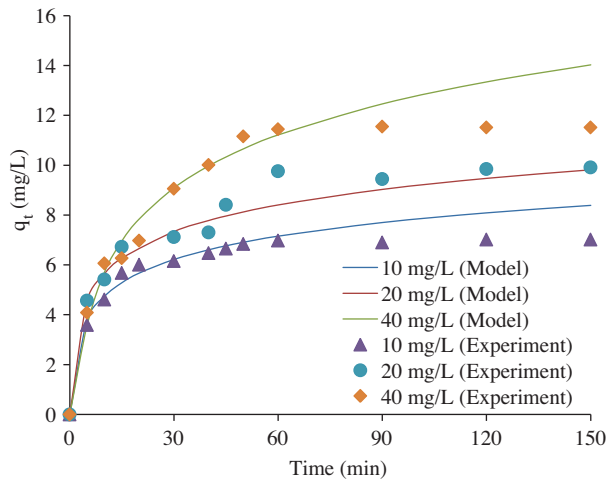

Figure 6. Pseudo-first-order kinetic model plots for adsorption of CV onto bottom ash (size = 75-150 μm).

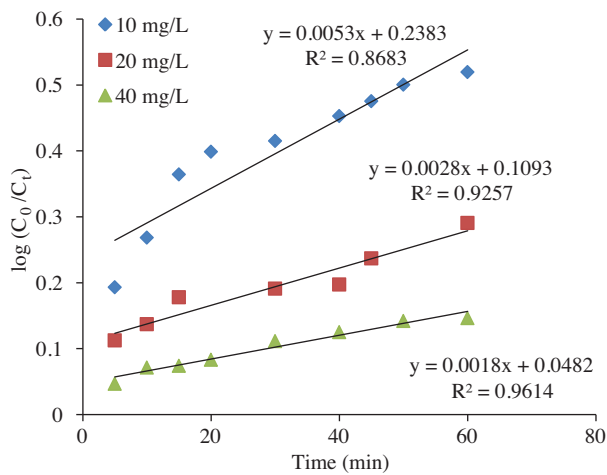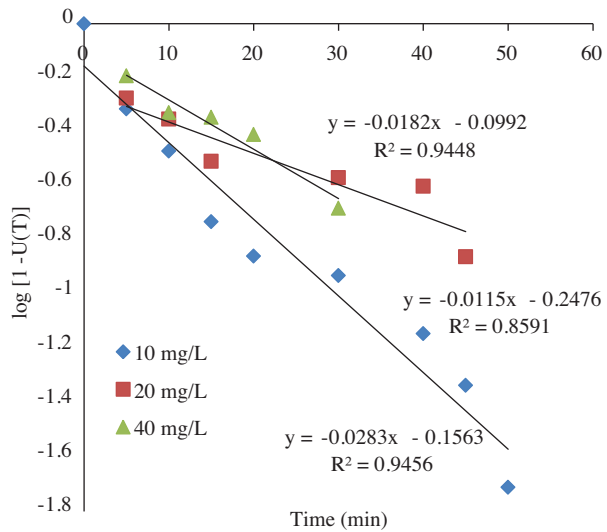**Figure 7.** Pseudo-second-order kinetic model plots for adsorption of CV onto bottom ash (size = 75-150 μm).
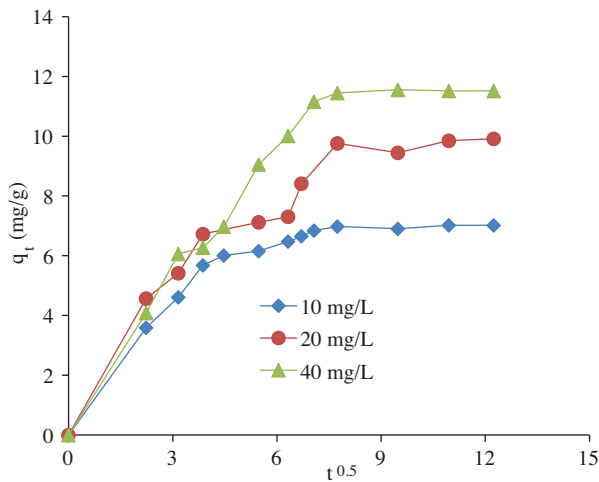
Figure 8. Intraparticle diffusion model plots for adsorption of CV onto bottom ash (size = 75-150 μm).

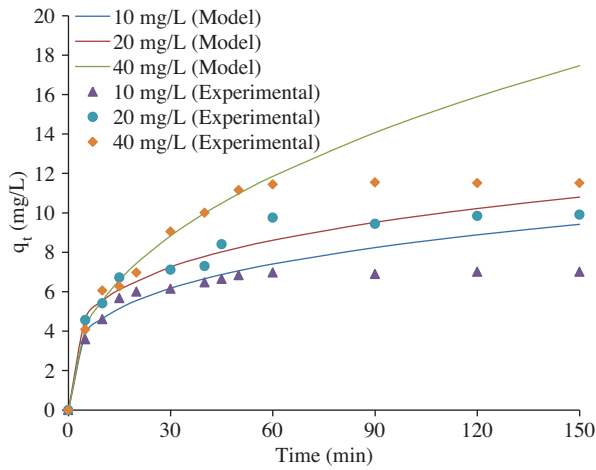**Figure 9.** Elovich model plots for adsorption of CV onto bottom ash (size = 75-150 μm).

Figure 10. Natarajan and Khalaf model plots for adsorption of CV onto bottom ash (size = 75-150 μm).


Figure 11. Bhattacharya and Venkobachar model plots for adsorption of CV onto bottom ash (size = 75-150 μm).

In order to identify the step governing the overall removal rate of the adsorption process, the model given by Boyd et al. (1947) and Reichenberg (1953) was applied (as per the procedure given by Gupta et al. (2004)) and the results are plotted as shown in Figure 14. The linearity test of Bt versus time plots was employed to distinguish between the film diffusion- and particle-diffusion-controlled adsorption. If the plot of Bt vs. time (having slope B) is a straight line passing through the origin, then the adsorption rate is governed by the particle diffusion mechanism; otherwise, it is governed by film diffusion (Singh et al., 2003). In the case of CV removal by bottom ash, an interesting nature of the plots was obtained. The plot of Bt vs. time is valid for both cases. This phenomenon suggests involvement of particle diffusion and film diffusion mechanisms as the rate-controlling step for removal of CV by bottom ash.

Figure 12. Power function kinetic model plots for adsorption of CV onto bottom ash (size = 75-150 μm).
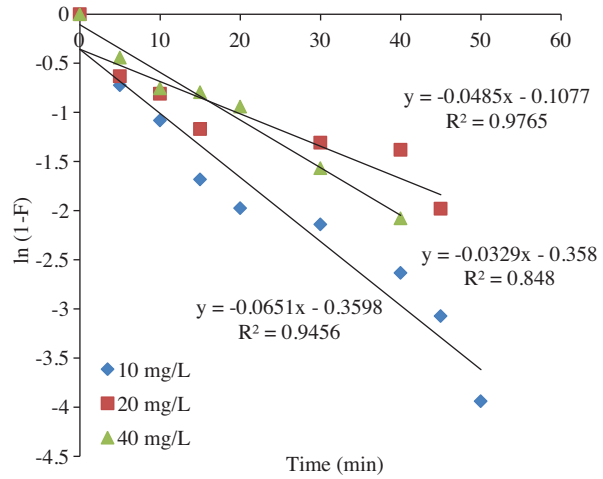

Figure 13. Film diffusion kinetic model plots for adsorption of CV onto bottom ash (size = 75-150 μm).
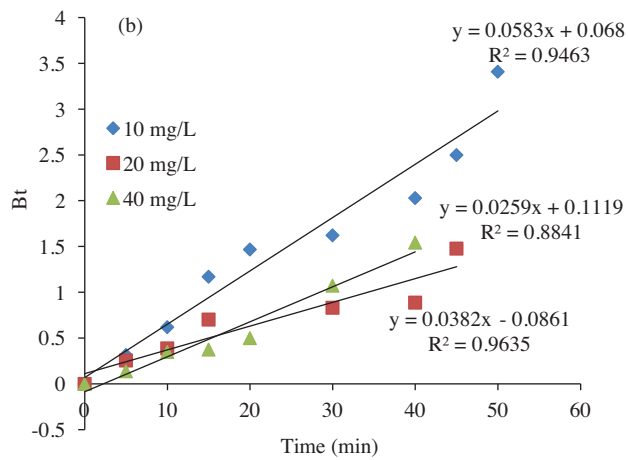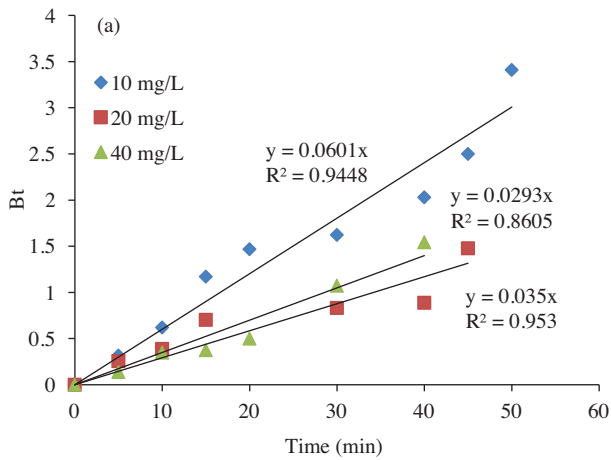
Figure 14. Time vs. Bt plot at different concentrations of CV (a) origin as intercept (b) nonzero intercept.

3.4. Effect of particle size

To illustrate the effect of the bottom ash particle size on CV adsorption, 4 ranges of particle size distribution, <75, 75-150, 150-300, and 300-600 μm, were used and the results are shown in Figure 15. The amount of CV adsorbed increases with the decrease in particle size of the adsorbent. The adsorption efficiency of bottom ash decreased from 89.85% to 23.1% as the particle size increased from <75 to 300-600 μm. This can be attributed to the fact that the smaller adsorbent particles have shortened diffusion paths and increased total surface area, and therefore the ability to penetrate all internal pore structures of adsorbent is very high (Gupta et al., 2009). It can also be seen from Figure 15 that the equilibrium time is almost constant for all sizes of bottom ash. From this it can be concluded that the equilibrium time is dependent on surface characteristics of the adsorbent and adsorbate and independent of adsorbent size.
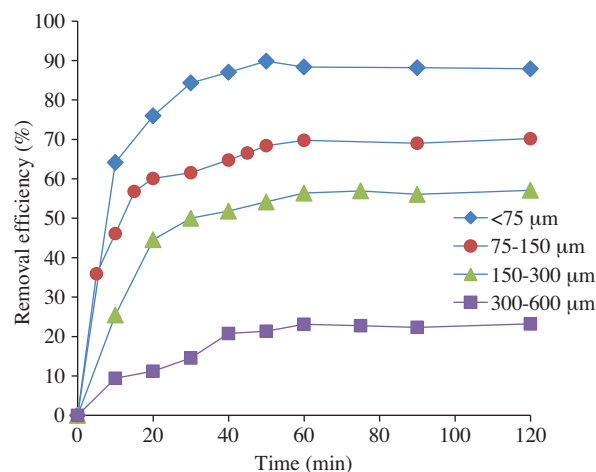
Figure 15. Effect of bottom ash particle size on CV adsorption.

The experimental results were also applied to the kinetic models and parameters of all models are given in Table 2. All the models fit well for experimental data. Pseudosecondorder kinetics follows the removal of CV by bottom ash for smaller particle size (<150 μm) but the kinetics follows first order in case of bottom ash size >150 μm. Since intraparticle diffusion plots do not pass through the origin, there should be some degree of boundary layer control and intraparticle diffusion is not the only rate-limiting step, but also other kinetic models may control the rate of adsorption, all of which may be operating simultaneously. The values of intercept give an idea about the boundary layer thickness, such as the larger the intercept the greater the boundary layer effect (Weber and Morris, 1963). Theoretically, the k_{id} and the adsorption capacity are related to available adsorbent surface area. For a spherical adsorbent particle and for a given mass of adsorbent, the total surface area is inversely proportional to the adsorbent particle diameter. Therefore, if only surface adsorption sites were utilized for dye removal, adsorption capacity should be proportional to the inverse particle diameter, $1/d$, for a given adsorbent mass (Poots et al., 1976). The plot of rate parameter versus square inverse diameter did not give a straight line and the only conclusion is that the intraparticle diffusion was not the only operative mechanism (Ghouti et al., 2009). Other models also follow the same trend as described earlier.

3.5. Effect of ionic strength

Wastewater containing dye commonly has higher salt concentration, and the effects of ionic strength are of some importance in the study of dye adsorption onto adsorbents (Han et al., 2007). Figure 16 shows the effect of various concentration of NaCl and $CaCl_2$ solution on bottom ash efficiency for an initial CV concentration of 10 mg/L and bottom ash dose of 0.5 g/L. Theoretically, when the electrostatic forces between the adsorbent surface and adsorbate ions are attractive, as in this system, an increase in ionic strength will decrease the adsorption capacity. Conversely, when the electrostatic attraction is repulsive, an increase in ionic strength will increase adsorption (Newcombe and Drikas, 1997; Alberghina et al., 2000; German-Heins and Flury, 2000). The experimental data from this study did not follow this convention, as the adsorption of positively charged CV molecules on negatively charged bottom ash increased with NaCl and $CaCl_2$ addition. The significant increase in dye removal after NaCl and $CaCl_2$ addition can be attributed to an increase in dimerization of CV in solution (Al-Degs et al., 2008). A number of intermolecular forces have been suggested to explain this aggregation; these forces include van der Waals forces, ion-dipole forces, and dipole-dipole forces, which occur

between dye molecules in the solution. It has been reported that these forces increased upon the addition of salt to the dye solution (Alberghina et al., 2000). Accordingly, the higher adsorption capacity of CV under these conditions can be attributed to the aggregation of dye molecules induced by the action of salt ions, i.e. salt ions force dye molecules to aggregate, increasing the extent of sorption on the bottom ash surface. Al Degs et al. (2008) and German-Heins and Flury (2000) have reported an increase in reactive dye adsorption after adding salt to the solution.
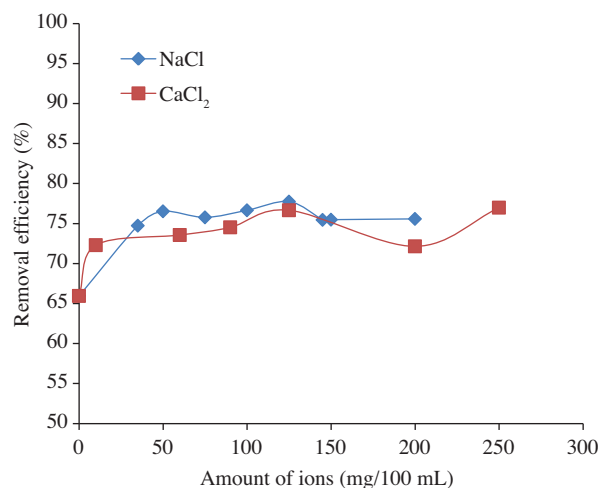
Figure 16. The effect of NaCl and CaCl$_2$ concentration on CV removal by bottom ash.

4. Conclusions

The bottom ash employed in the adsorption processes is efficient in removing CV from aqueous solutions. The adsorption capacity of bottom ash is influenced by contact time, initial CV concentration, particle size, and ionic strength. All the kinetic models fit the experimental data well. The kinetic modeling study has shown that the experimental data followed the pseudo-second-order model for bottom ash size <150 μm and pseudo-first-order model for higher sizes, suggesting a multistep process. There is a significant contribution of intraparticle diffusion and film diffusion in CV removal by bottom ash. The adsorption capacity of bottom ash decreases with increase in CV concentration and increases with particle size. The significant increase in dye removal after NaCl and CaCl$_2$ addition can be attributed to an increase in dimerization of CV in solution.

References

Adak, A., Bandyopadhyay, M. and Pal, A., "Removal of Crystal Violet Dye from Wastewater by Surfactant-Modified Alumina", Separation and Purification Technology, 44, 139-144, 2005.

Alberghina, G., Bianchini, R., Fichera, M. and Fisichella, S., "Dimerization of Cibacron Blue F3GA and Other Dyes: Influence of Salts and Temperature", Dyes and Pigments, 46, 129-37, 2000.

Al-Degs, Y.S., El-Barghouthi, M.I., El-Sheikh, A.H. and Walker, G.M., "Effect of Solution pH, Ionic Strength, and Temperature on Adsorption Behavior of Reactive Dyes on Activated Carbon", Dyes and Pigments, 77, 16-23, 2008.

Al-Ghouti, M.A., Khraisheh, M.A.M., Ahmad, M.N.M. and Allen, S., "Adsorption Behaviour of Methylene Blue onto Jordanian Diatomite: A Kinetic Study", Journal of Hazardous Materials, 165, 589-598, 2009.

Banat, I.M., Nigam, P., Singh, D. and Marchant, R., "Microbial Decolorization of Textile-Dye-Containing Effluents: A Review" Bioresour. Technol., 58, 217-227, 1996.

Bayat, B., "Comparative Study of Adsorption Properties of Turkish Fly Ashes. I. The Case of Nickel (II), Copper (II) and Zinc (II)", Journal of Hazardous Materials, B95, 251273, 2002.

Bello, O.S., Adelaide, O.M., Hammed, M.A. and Popoola, O.A.M., "Kinetic and Equilibrium Studies of Methylene Blue Removal from Aqueous Solution by Adsorption on Treated Sawdust", Macedonian Journal of Chemistry and Chemical Engineering, 29, 77-85, 2010.

Benfield, L.D., Weand, B.L. and Judkins, J.F., Process Chemistry for Water and Wastewater, Prentice Hall Inc, Englewood Cliffs, New Jersey, 1982.

Bhattacharya, A.K. and Venkobachar, C., "Removal of Cadmium by Low Cost Adsorbents", Journal of Environmental Engineering, 110, 110-116, 1984.

Boyd, G.E., Adamson, A.W. and Myers, L.S. "The Exchange Adsorption of Ions from Aqueous Solutions by Organic Zeolites, II, Kinetics", Journal of the American Chemical Society, 6911, 2836-2848, 1947.

Chien, S.H. and Clayton, W.R., "Application of Elovich Equation to the Kinetics of Phosphate Release and Sorption on Soils", Soil Science Society of America Journal, 44, 265-268, 1980.

Crini, G., "Non-Conventional Low-Cost Adsorbents for Dye Removal: A Review", Bioresource Technology, 97, 1061-1085, 2006.

Dalal, R.C. "Desorption Of Phosphate by Anion Exchange Resin", Communications in Soil Science and Plant Analysis, 5, 531-538, 1974.

Derbyshire, F., Jagtoyen, M., Andrews, R., Rao, A., Martin-Gullon, I. and Grulke, E., Carbon Materials in Environmental Applications. In: Radovic, L.R. Ed., Chemistry and Physics of Carbon. Marcel Dekker, New York, 27, 1–66, 2003.

German-Heins, J. and Flury, M., "Sorption of Brilliant Blue FCF in Soils as Affected by pH and Ionic Strength", Geoderma, 97, 87-101, 2000.

Gong, R.M., Li, M., Yang, C., Sun, Y.Z. and Chen, J., "Removal of Cationic Dyes from Aqueous Solution by Adsorption on Peanut Hull", Journal of Hazardous Materials, B 121, 247-250, 2005.

Gupta, V.K., Mittal, A., Krishnan, L. and Gajbe, V., "Adsorption Kinetics and Column Operations for the Removal and Recovery of Malachite Green from Wastewater Using Bottom Ash", Separation and Purification Technology, 40, 87-96, 2004.

Gupta, V.K., Mittal, A., Malviya, A. and Mittal, J. "Adsorption of Carmoisine A from Wastewater using Waste Materials—Bottom Ash and Deoiled Soya", Journal of Colloid and Interface Science, 335, 2433, 2009.

Han, R., Zou, W., Yu, W., Cheng, S., Wang, Y. and Shi, J., "Biosorption of methylene blue from aqueous solution by fallen phoenix tree's leaves", Journal of Hazardous Materials, 141, 156-162, 2007.

Hecht, N.L. and Duvall, D.S., Characterization and Utilization of Municipal and Utility Sludges and Ashes, vol. III, Utility Coal Ash, National Environmental Research Center, US Environmental Protection Agency, 1975.

Hema, M. and Arivoli, S., "Comparative Study on the Adsorption Kinetics and Thermodynamics of Dyes onto Acid Activated Low Cost Carbon", International Journal of Physical Sciences, 21, 010-017, 2007.

Ho, Y.S. and McKay, G. "Pseudo-Second-Order Model for Sorption Processes", Process Biochemistry, 34, 451465, 1999.

Ho, Y.S. and McKay, G., "Sorption of Dyes and Copper Ions onto Biosorbents", Process Biochemistry, 38, 1047-1061, 2003.

Jain, A.K., Gupta, V.K., Bhatnagar, A. and Suhas, "Utilization of industrial waste products as adsorbents for the removal of dyes", Journal of Hazardous Materials, B101, 31-42, 2003.

Kannan, N. and Vanangamudi, A., "A Study on Removal of Chromium VI by Adsorption on Lignite Coal", Indian Journal of Environmental Protection, 114, 241-245, 1991.

Lagregren, S., "About the Theory of So-Called Adsorption of Soluble Substances", Kungliga Svenska Vetenskap-sakademiens Handlinga, 24, 139, 1898.

Lin, J.X., Zhan, S.L., Fang, M.H. and Qian, X.Q., "The Adsorption of Dyes from Aqueous Solution Using Diatomite" Journal of Porous Materials, 14, 449455, 2007.

McKay, G., Porter, J.F. and Prasad, G.R., "The Removal of Dye Colours from Aqueous Solutions by Adsorption on Low-Cost Materials", Water Air Soil Pollution, 114, 423-438, 1998.

McMullan, G., Meehan, C., Conneely, A., Kirby, N., Robinson, T., Nigam, P., Banat, I.M., Marchant, R. and Smyth, W.F., "Microbial Decolourisation and Degradation of Textile Dyes", Applied Microbiology and Biotechnology, 56, 81-87, 2001.

Mittal, A., Mittal, J., Malviya, A., Kaur, D. and Gupta, V.K. "Adsorption of Hazardous Dye Crystal Violet from Wastewater by Waste Materials", Journal of Colloid and Interface Science, 343, 463473, 2010.

Newcombe, G. and Drikas, M., "Adsorption of NOM Activated Carbon: Electrostatic and Non-Electrostatic Effects", Carbon, 35, 1239-50, 1997.

Nidheesh, P.V., Gandhimathi, R., Ramesh, S.T. and Anantha Singh, T.S., "Investigation of Equilibrium and Thermodynamic Parameters of Crystal Violet Adsorption onto Bottom Ash", J. Int. Environmental Application & Science, 6, 461-470, 2011.

Oladoja, N.A. and Aliu, Y.D. "Snail Shell as Coagulant Aid in the Alum Precipitation of Malachite Green from Aqua System", Journal of Hazardous Materials, 164, 1496-1502, 2009.

Padmesh, T.V.N., Vijayaraghavan, K., Sekaran, G. and Velan, M., "Biosorption of Acid Blue 15 using Fresh Water Macroalga Azolla Filiculoides: Batch and Column Studies", Dyes and Pigments, 71, 77-82, 2006.

Poots, V.J.P., McKay, G. and Healy, J.J., "The Removal of Acid Dye from Effluent using Natural Adsorbent-I Peat", Water Research, 10, 1061-1066, 1976.

Reichenberg, D., "Properties of Ion-Exchange Resin in Relation to Their Structure. III. Kinetics of Exchange", Journal of the American Chemical Society, 75, 589, 1953.

Robinson, T., McMullan, G., Marchant, R. and Nigam, P., "Remediation of Dyes in Textile Effluent: A Critical Review on Current Treatment Technologies with a Proposed Alternative", Bioresource Technology, 77, 247-255, 2001.

Singh, K.P., Mohan, D., Sinha, S., Tondon, G.S. and Gosh, D., "Color Removal from Wastewater using Low-Cost Activated Carbon Derived from Agricultural Waste Material", Industrial & Engineering Chemistry Research, 42, 1965-1976, 2003.

Song, J.Y., Zou, W.H., Bian, Y.Y., Su, F.Y. and Han, R.P., "Adsorption Characteristics of Methylene Blue by Peanut Husk in Batch and Column Modes", Desalination, 265, 119-125, 2011.

Tan, I.A.W., Ahmad, A.L. and Hameed, B.H. "Adsorption of Basic Dye Using Activated Carbon Prepared from Oil Palm Shell: Batch and Fixed Bed Studies", Desalination, 225, 13-28, 2008.

Vaghetti, J.C.P., Lima, E.C., Royer, B., Cardoso, N.F., Martins, B. and Calvete, T., "Pecan nutshell as biosorbent to remove toxic metals from aqueous solution", Separation Science and Technology, 44, 615-644, 2009.

Weber, W.J. and Morris, J.C. "Kinetics of Adsorption on Carbon from Solution", Journal of Sanitary Engineering Division, American Society of Chemical Engineers, 89, 31-59, 1963.

Weng, C.H. and Pan, Y.F., "Adsorption of A Cationic Dye Methylene Blue onto Spent Activated Clay", Journal of Hazardous Materials, 144, 355-362, 2007.

Xing, Y., Liu, D. and Zhang, L.P., "Enhanced Adsorption of Methylene Blue by EDTAD-Modified Sugarcane Bagasse and Photocatalytic Regeneration of the Adsorbent", Desalination, 259, 187-191, 2010.